Radiation-sensitivity enhancement and annealing variation in densified, amorphous SiO_2

R. A. B. Devine
Centre National d'Etudes des Télécommunications, Boîte Postale 98, 38243 Meylan, France
(Received 28 January 1987)

The influence of ^{60}Co γ radiation on densified samples of wet and dry amorphous silica has been studied through the creation and annealing of three intrinsic defects. Radiation sensitivity for oxygen-vacancy creation is enhanced by nearly 2 orders of magnitude in samples densified by only 3%. In general, defect creation efficiency is three to four times larger in wet silica than in dry both in the densified and undensified forms. Diffusion or thermal detrapping models for oxygen-vacancy annealing both suggest the activation energy for annealing increases by 0.6 to 1.0 eV when samples are densified by $\sim 16\%$. Creation of the peroxy radical through transformation of oxygen-vacancy centers is discussed.

INTRODUCTION

In 1953 Primak and co-workers[1] demonstrated that exposure of vitreous silica (a-SiO_2) in a nuclear reactor resulted in a permanent densification of the silica which they attributed to the fast neutrons. Extensive subsequent studies indicated[2] that similar densification of silica could be produced by other energetic species such as ions and electrons, and these at energies where the primary mechanism of energy loss is through ionization phenomena rather than collisional, atomic displacement. A bond-cleavage model was proposed to explain the observed densification in which it was assumed that Si—O linkages were broken by the incident radiation, O or Si atoms were displaced, and a thermally stimulated restructuring of the lattice occurred. The final state is clearly denser than the initial. Further studies[3] using low-energy electrons ($\lesssim 18$ keV) and charged ions (Ar^{2+}, H^+, He^+) to irradiate thin films of amorphous SiO_2 produced by oxidation of Si, indicated that a maximum, stable densification of $\sim 3\%$ could be obtained for an energy deposition of $\sim 2\times 10^{23}$ keV/cm^3 into ionizing processes or 2×10^{20} keV/cm^3 into atomic displacement. The latter result clearly demonstrates the efficiency of the displacement process as compared to ionization and reinforces the bond cleavage spike hypothesis. In the absence of detailed structural information on the densified state, it is interesting to ask whether or not defect creation alone (absence of structural recombination) might account for the observed densification. Recent studies[4] may be used to provide an answer. Using energies similar to those used in the densification studies,[3] it was found that the most common defect, the oxygen vacancy center,[5] observed in a-SiO_2 was produced with an efficiency of 2×10^{13} defects/cm^3 Mrad. Assuming a fractional volume decrease[3] of 0.34% is induced by 10^5 Mrad, one concludes that each defect would be responsible for the volume collapse of ~ 40 SiO_2 molecules. Clearly such a change is unrealistic and restructuring arguments are indeed more plausible.

Stress measurements on thin films[3] subjected to irradiation where collisional processes are the primary source of energy loss suggest that after irradiation there is a maximum stress in the films of ~ 10 kbar. Neutron irradiation results[6] on vitreous silica indicate a maximum densification in collisional processes of $\sim 2.8\%$, so that combining these two figures one deduces $(\Delta V/V)/\Delta p = -0.28\%$/kbar *on the assumption that the residual stress has produced the densification.* It turns out that this result is close to that obtained from pressure-volume measurements[7] on vitreous silica performed in the reversible range. The densification produced by irradiation is, however, metastable and can only be removed by annealing at temperatures >800 °C. Furthermore, from pressure-volume studies[8,9] it is well known that metastable densification of amorphous SiO_2 occurs only for pressures in excess of ~ 80 kbar at room temperature. Consequently, the densification of amorphous SiO_2 due to particle irradiation cannot be attributed to the residual stress left in the film but in fact appears due to some structural effect during the irradiation. This conclusion fully supports the bond-cleavage spike model.

As a result of such considerations as those enumerated above the physical nature of amorphous SiO_2 in the elastic and plastic (metastable) states has been the subject of growing interest. On a microscopic scale it is extremely difficult to imagine an experiment which will provide information on an atomic dimension. Currently, the most exploited technique appears to be Raman scattering where the various peaks observed in the Raman spectrum are identified with the different modes of vibration of the SiO_2 network. It has been clearly demonstrated that if pressures >80 kbar are applied at room temperature, a remnant densification remains when the pressure is relaxed.[8–10] Pressures less than 80 kbar at elevated temperatures (>300 °C) result in a remnant densification when the pressure and temperature are relaxed.[11] Detailed analysis[10] of the Raman spectra both in the reversible phase of densification and in the irreversible or metastable phase suggests that, under pressure, the mean Si—O—Si bond angle θ decreases, while the dihedral angle (relative rotation of adjoining SiO_4 tetrahedral) δ and the mean Si—O bond length r both increase. These results are consistent with the conclusions of x-ray diffraction studies on

single-crystal quartz under hydrostatic pressure[12], and the reduction in θ is also consistent with x-ray scattering[13] and nuclear-magnetic-resonance results[14] on metastable, densified amorphous SiO_2. Differences observed in the Raman spectra in the elastic and plastic deformation regimes[9,10] appear to indicate an increase in intensity of certain peaks associated with the presence of low-member rings (three and four) of SiO_4 tetrahedra, suggesting that a change in the distribution of ring statistics may have occurred in the metastable phase.[15] Similar conclusions may be drawn from the Raman spectra obtained on densified a-SiO_2 produced by neutron bombardment.[16]

The physical difference between a-SiO_2 densified in the reversible regime and that densified in the irreversible regime and by neutron bombardment would appear to be related to an internal structure modification of the ring statistics. The nature of the network modifications can be hypothesised if we recall that SiO_2 is composed of a wide distribution of ring statistics and that the Si—O—Si bond angle is a rather insensitive function[17] of energy per molecule, i.e., for $120° < \theta < 180°$ the binding energy per molecule of SiO_2 varies by only 0.2 eV. Low-energy "elastic" variations can then be thought of as brought about by puckering of large-membered rings, leading to a reduced mean Si—O—Si bond angle. A "metastable" reduction in bond angle may be brought about by subdivision of large-member rings into numerous small-member rings.[18] Such a process would appear to be intuitively metastable.

The foregoing discussion emphasizes the fact that at present very little is known about the nature of densified forms of a-SiO_2 apart from some information on a rather macroscopic scale. In a recent preliminary study[19] we endeavored to gain some insight into the structural modifications and variations in physical properties of densified silica by studying the creation and annihilation dynamics of defects produced in Suprasil W1 by γ irradiation before and after densification. In particular, the annealing dynamics of oxygen-vacancy centers[5] (E_1') and peroxy radicals[20] were studied in a sample densified by $\sim 13\%$, and it was found that the oxygen vacancies anneal out at temperatures significantly higher than in undensified silica. Coincidently, the peroxy radicals formed at higher temperatures, emphasizing the 1:1 correspondence between these two intrinsic defects.[20] The following work reports the results of much more detailed studies on defects in undensified and densified silica. We have studied defect creation efficiency as a function of densification and of silica type (wet or dry) and have studied isochronal and isothermal annealing curves.

EXPERIMENT AND RESULTS

Samples used in these experiments were cut from commercially available wet (Suprasil I) and dry (Suprasil W1) silica rods obtained from Heraeus Schott Quartzschmeltze. Densification was carried out using a belt apparatus[11] with silver chloride as the pressure-transmitting medium. In Table I we list the samples studied, the densification conditions, the resultant density, and the densification percentage. Densities were measured using the floatation technique.[11] Irradiation of samples was carried out at room temperature using a ^{60}Co source of γ rays at a rate of 0.8 Mrad/h. Accumulated doses of 76 Mrad were used. Following irradiation, both before and after annealing, samples were stored under liquid nitrogen to avoid any possible room-temperature annealing. Electron-spin-resonance measurements were carried out using a Bruker ER 200 D X band spectrometer with variable temperature facility. A small Cr^{3+}-in-MgO sample was left permanently in the microwave cavity both to serve as a g marker ($g = 1.9799$) and as a control of the spectrometer against fluctuation such as loaded Q variation, power fluctuation, etc. The density of defects was estimated by recording the spectra at low magnetic field

TABLE I. Conditions of pressure, temperature and time used to obtain the samples studied in this work. Also quoted are the measured densities (by floatation methods), and the densification percentages.

Densification condition				
Pressure (kbar)	Time (min)	Temperature (° C)	Density (g/cm^3)	Densification (%)
	Suprasil I		2.202	0
50	3	600	2.316	5.2
50	5	500	2.424	9.2
50	8	575	2.535	15.1
85	15	710	2.567	16.5
120	30	900	2.731	24.0
	Suprasil W1			
50	0[a]	500	2.267	3.0
50	0[a]	500	2.366	7.5
50	12	450	2.422	9.9
50	7	600	2.492	13.1
50	7	600	2.544	16.0

[a]These samples were simply heated to the densification temperature then cooled immediately, leaving no dwell time at high temperature.

modulation levels (100 kHz, 0.2 G peak to peak) and comparing the intensity of the absorption curve obtained by double integration with that from a standard sample containing a predetermined number of spins (strong pitch) run under identical experimental conditions. Automatic baseline adjustment was performed to minimize integration errors. The spectra of the oxygen-vacancy (E_1') centers were recorded at room temperature using incident microwave power levels of the order of 2 μW. Peroxy-radical and nonbridging oxygen hole (NBOH) centers were studied at 120 K using incident microwave power levels of 2 mW and a magnetic field modulation amplitude of 2.0 G peak to peak. Under these power conditions the resonance spectra measured did not show saturation effects.

We have examined the creation and annealing behavior of the three intrinsic structural defects, the E_1' center ($Si^+ \cdot Si$), the peroxy radical (Si—O—O$\cdot$), and the NBOH center (Si—O$\cdot$). We will deal with the results obtained in turn.

E_1' center

In Fig. 1 we show the E_1' resonance spectra obtained in undensified Suprasil I [Fig. 1(a)], 15% densified Suprasil I [Fig. 1(b)], and 24% densified Suprasil I [Fig. 1(c)]. The line-shape variations observed in Suprasil W1 for the same densifications were identical within experimental error. By double-integration methods and by comparison with the strong pitch reference, we acertain that under the same irradiation conditions (76 Mrad, ^{60}Co γ rays) a defect density N of 3.3×10^{17} defects/cm^3 is created in a Suprasil W1 sample densified by 10%, and 4.4×10^{15} defects/cm^3 in an undensified sample. In Suprasil I densified by 10% the defect density was 1.1×10^{18} defects/cm^3 and 1.6×10^{16} defects/cm^3 in the undensified case. The absolute accuracy of these values is of the order of 50% but the relative values are accurate to better than 10%. If we compare the relative defect creation efficiencies (C) between Suprasil I and W1, the ratio $[C(I)/C(W1)]$ is 3.6 for the undensified case and 3.2 for the 10% densified case. The spin density found in undensified Suprasil I was in excellent agreement with that found by other workers[21] who used approximately 4 times the accumulated dose we used (after scaling down their density to allow for this).

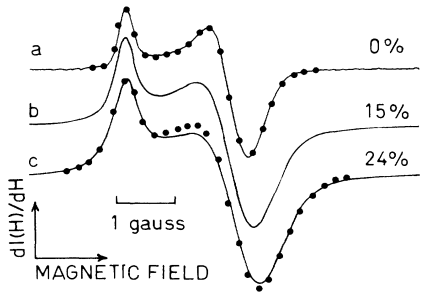

FIG. 1. Experimental absorption derivative electron-spin-resonance line shapes observed for the E_1' defect in samples of Suprasil I after irradiation with 76 Mrad of ^{60}Co γ rays. The three curves correspond to different densifications of the Suprasil I. The filled circles show the fits to the curves obtained as explained in the text using parameter values quoted in Table II.

The experimental line shapes shown in Fig. 1 were analyzed using a computer-fitting procedure in which the absorption line shapes $I(H)$, as a function of magnetic field H, are given by

$$I(H)=\sum_{g_1,g_2,g_3}\sum_{\theta,\phi}p(g_1)p(g_2)p(g_3)\times F(H,g(g_1,g_2,g_3,\theta,\phi)) , \quad (1)$$

with

$$g=(g_3^2\sin^2\theta\sin^2\phi+g_2^2\sin^2\theta\cos^2\phi+g_1^2\cos^2\theta)^{1/2} .$$

θ and ϕ are the angles between the applied field and the principal axes of the SiO_4 tetrahedron. Angular summation allows for the random distribution of angles anticipated in the amorphous solid. The shape function F at each g value was assumed to be Lorentzian, while the probability amplitudes for the three principal g factors, $p(g_i)$, were taken as Gaussian. Fits to the experimental line shapes for undensified and 24% densified Suprasil I are shown by the filled circles in Fig. 1. The relevant fit parameters are given in Table II. The fit is found to be very satisfactory in the undensified case but it becomes progressively difficult to obtain a satisfactory fit as the sample density is increased. Note that both the g factor spread Δg_i and the intrinsic absorption linewidths ΔH_L increase as the sample is densified. In the fit procedure for the undensified case, contrary to common practice,[21] we assumed an intrinsic linewidth equal to that of single-crystalline quartz and then adjusted the g-factor spread values to obtain the best fit. We note, as one would expect, that the spread of g factors is much larger in g_2 and g_3 than in g_1.

From the spin-density measurements cited above we can estimate the influence of dipolar (spin-spin) broadening on the measured linewidths. Assuming the dipolar absorption linewidth broadening is given by[22]

$$\Delta H_{DD}=2.3g\beta N[S(S+1)]^{1/2} ,$$

and taking $g=2.0$, $S=\frac{1}{2}$, we estimate that a defect density of 10^{18} defects/cm^3 would result in a ΔH_{DD} of 50 mG. From Table II we see that the increase in absorption linewidth required to fit the data on samples densified by 15% is 160 mG, so that simple dipolar broadening arguments cannot account for the total increase in linewidth.

In Fig. 2 we present the results of defect-creation efficiency measurements in densified Suprasil I and Suprasil W1 as a function of densification. We compare the efficiencies of creation by 76 Mrad of ^{60}Co γ rays with respect to the undensified case and consequently show the ratio. We observe that even for a sample densified by only 3%, the E_1' defect creation efficiency is 60 times that found in undensified silica of the same type.

Isochronal and isothermal anneals were carried out on

TABLE II. Summary of the parameters required to give a best fit of the derivative of the line-shape equation (1) to the data shown in Fig. 1. A Gaussian distribution of g factors about the principal values (g_1,g_2,g_3) was assumed together with a Lorentzian line-shape function $F(H,g)$.

Densification of sample (%)	g_1	g_2	g_3	Δg_1	Δg_2	Δg_3	ΔH_L (G)
0	2.001 53	2.000 22	2.000 07	0.000 08	0.000 25	0.000 25	0.1
15	2.001 53	2.000 16	2.000 03	0.000 08	0.000 39	0.000 29	0.26
24	2.001 53	2.000 12	2.000 00	0.000 11	0.000 47	0.000 32	0.32

various samples of densified Suprasil I and Suprasil W1. In Fig. 3 we show the results of 10-min isochronal anneals on Suprasil I densified by 16.5% (filled circles), Suprasil W1 densified by 16% (filled triangles), and Suprasil W1 densified by 9.9% (filled squares). For comparison we include the anneal curves obtained[23,24] for Suprasil W1 (solid line) and Suprasil I (dashed line) in the undensified states. Isothermal anneal results of measurements carried out on the 16.5% densified Suprasil I sample are shown in Fig. 4. We note that the anneal curves have the usual form of a rapid initial descent followed by a long tail which characterizes annealing processes where a range of activation energies is involved.[25]

NBOH and peroxy-radical centers

Measurements were carried out at 120 K to study the NBOH and peroxy-radical centers. Figure 5 shows a series of typical spectra obtained in undensified and densified forms of Suprasil I and Suprasil W1. The very intense central resonance shown off scale in Figs. 5(a), 5(b), 5(d), and 5(e) is the E_1' signal; its overmodulated form can still be seen in the 16.5% densified Suprasil I sample after annealing at 625 °C for 10 min [Fig. 5(f)]. The resonance is totally absent in densified Suprasil W1 subjected to a 10-min anneal at 600 C [Fig. 5(f)]. The high-field resonance shown in Fig. 5(a) is the Cr^{3+}-in-MgO marker resonance. We underline the fact that undensified Suprasil I [Fig. 5(a)], densified Suprasil I [Fig. 5(b)], and densified Suprasil W1 [Fig. 5(e)] all show the positive-going low-field peak attributed to the NBOH center (NBOHC).[26] The high-field negative-going peak is masked by the intense E_1' signal. In undensified Suprasil W1 [Fig. 5(d)], densified, annealed Suprasil I [Fig. 5(c)], and densified, annealed Suprasil W1 [Fig. 5(f)] we observe peaks associated with the peroxy radical.[26] Whereas both positive-going, low-field peaks of the NBOH center and the peroxy radical are observed in undensified Suprasil W1, only the peroxy peak remains in the densified, annealed samples of Suprasil W1 and Suprasil I.

We have followed the isochronal annealing of the NBOH center in the 16.5% densified Suprasil I sample by measuring the peak-to-peak amplitude of the low-field peak [A in Fig. 5(a)]. The results as a function of anneal temperature are shown in Fig. 6 together with results available[27] for undensified Suprasil I. Care must be taken in comparing these curves since we were unable to measure the complete shape of the NBOHC resonance due to the presence of the E_1' signal. Therefore we did not perform double integration of the line shape as is required if

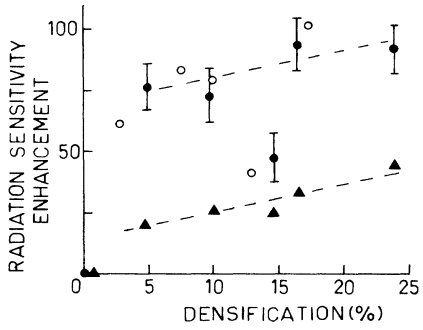

FIG. 2. Measured enhancement of the defect creation efficiency in densified samples as a function of densification prior to irradiation with 76 Mrad of ^{60}Co γ rays. Filled circles, E_1' defects in Suprasil I; open circles, E_1' defects in Suprasil W1; and filled triangles, NBOH centers in Suprasil I. The enhancement quoted is relative to the defect density in the undensified silica after the same irradiation.

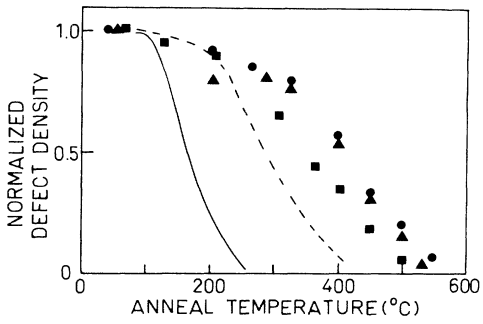

FIG. 3. Ten-minute isochronal annealing results for the E_1' defect density in different samples of densified silica: filled circles, Suprasil I densified by 16.5%; filled triangles, Suprasil W1 densified by 16%; filled squares, Suprasil W1 densified by 9.9%. The solid line is the annealing curve found in undensified Suprasil W1 while the dashed curve is that found in undensified Suprasil I.

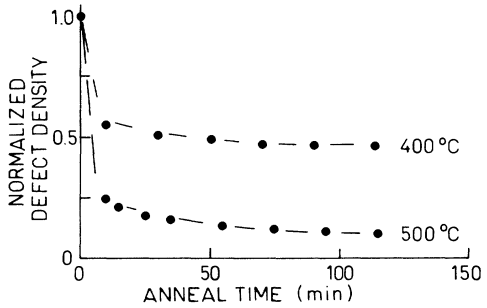

FIG. 4. Isothermal annealing curves at 400 °C and 500 °C for E_1' defects in the sample of 16.5% densified Suprasil I.

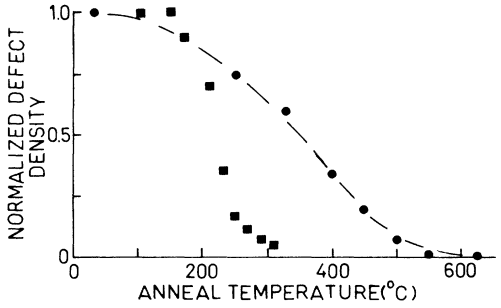

FIG. 6. Ten-minute isochronal annealing results on Suprasil I samples irradiated with 76 Mrad of ^{60}Co γ rays prior to annealing. The full circles correspond to samples densified by 16.5% and correspond to the height A indicated in Fig. 5(a). The filled squares are data taken from Ref. 27 for samples irradiated at 77 K with 1.5×10^6 rad of 100-keV x rays.

the line shape varies. Figure 6 is plotted under the assumption of invariant line shape. It would appear from Fig. 6 that higher temperatures are required to anneal the NBOH centers in densified silica consistent with the behavior observed for the E_1' annealing shown in Fig. 3.

We have included in Fig. 2 (filled triangles) the ratio of the creation efficiencies of the NBOH centers in densified and undensified Suprasil I as a function of densification. Again, densification appears to produce an enhancement in the defect creation efficiency for a given γ dose. We have not plotted the result appropriate to Suprasil W1 because, as seen in Fig. 5(d), extraction of the NBOHC signal amplitude is rendered very difficult by the simultaneous presence of the peroxy radical and E_1' signals.

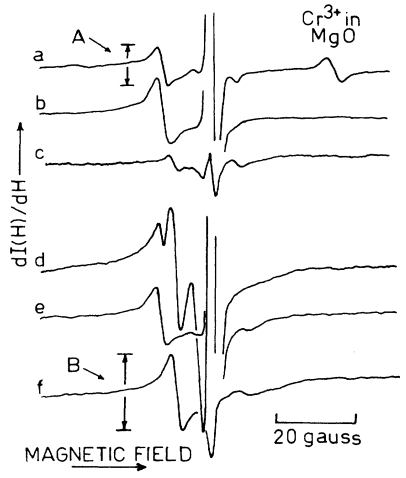

FIG. 5. Typical experimental line shapes of the absorption derivative observed in different samples at 120 K. Curve a undensified Suprasil I after 76 Mrad of ^{60}Co γ rays; curve b, 16.5% densified Suprasil I after irradiation; curve c, 16.5% densified Suprasil I after irradiation then annealing at 625 °C for 10 min; curve d, undensified Suprasil W1 after irradiation; curve e, 16% densified Suprasil W1 after irradiation; curve f, 16% densified Suprasil W1 after irradiation then annealing for 10 min at 600 °C. A on curve a indicates peak height used to characterize NBOH center. B on curve f denotes the height used to characterize the amplitude of the peroxy-radical signal.

We have followed the evolution of the peroxy radical in Suprasil W1 samples densified by 16% and 9.9% as a function of 10-min anneals at different temperatures. The resultant peak-to-peak amplitude [B in Fig. 5(f)] as a function of anneal temperature is given in Fig. 7. We also include data[25,28] on peroxy annealing in undensified Suprasil W1. Consistent with the behavior of the E_1' and NBOH-center defects, higher temperatures are required for annealing in the densified case than in the undensified case. The optimum temperature for transformation appears to shift from ~300 °C in undensified Suprasil W1 to ~530 °C in the densified form. Attention is drawn to the comparison between Figs. 3 and 7. We note that the E_1' resonance dissappears as the peroxy-radical resonance appears in Suprasil W1 in both the undensified and densified forms in strong support of the model of correlated annealing.[20] In Suprasil I the peroxy-radical resonance is also found to maximize around 550 °C, however, the interfer-

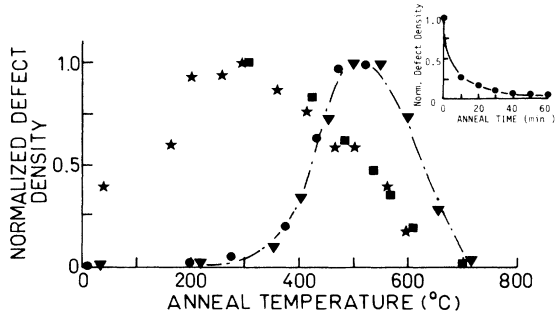

FIG. 7. Ten-minute isochronal annealing curves for peroxy-radical defects in different Suprasil W1 samples. Filled stars, undensified (Ref. 28); filled squares, undensified samples after preliminary annealing at 300 °C for 1 h prior to subsequent annealing (Ref. 25); filled circles, 16% densified samples; filled inverted triangles, 9.9% densified samples. The inset shows the isothermal annealing of the 9.9% sample annealed at 650 °C. The parameter used to characterize the defect density is the height B shown in Fig. 5(f).

ence of the NBOH-center resonance signal renders it impossible to get accurate estimates of the annealing curve. We show in the inset of Fig. 7 the isothermal annealing data on the peroxy signal in the 9.9% densified sample at one temperature, 650 °C. The decrease in signal amplitude is not exponential but tends towards the long-tailed curve as encountered for the E_1' resonance in Fig. 4 and the curve for peroxy annealing[25] in undensified Suprasil W1. Straightforward comparison is not possible because peroxy radicals clearly result from a thermally activated conversion process, and to perform proper annealing studies it would have been necessary to begin after assuring total conversion of all the peroxy precursors.

DISCUSSION

We will consider first the results of annealing studies on E_1' centers in undensified and densified Suprasil. It has been predicted[20] that in dry silica (Suprasil W1) oxygen-vacancy centers anneal via the trapping of diffusing, molecular oxygen to form peroxy radicals. As demonstrated by the correlation in the two annealing curves in Figs. 3 and 7, the peroxy-radical density indeed grows as the E_1' density decreases both in the densified and undensified forms. If we compare the shift in temperature of the annealing curves resulting from densification we note that the temperature at which the E_1' density falls to half its initial value rises from 160 °C in undensified silica to 420 °C in the densified case, i.e., a rise of 260 °C. At the same time, the temperature at which the peroxy-radical signal growth is maximized rises from 300° to 530 °C, i.e., an increase of 230 °C. The similarity of these two figures quantitatively supports the idea of correlated peroxy-radical growth and E_1' annealing. Absolute defect density determinations performed on one sample[19] also demonstrated that the peroxy-radical density after annealing was equal within experimental error to the E_1' density prior to annealing. In dry silica, it would appear then that E_1' annealing takes place via trapping of O_2:

$$\equiv \mathrm{Si}^{\cdot} + \mathrm{O_2} \rightleftarrows \equiv \mathrm{Si{-}O{-}O}^{\cdot} \ . \tag{2}$$

On this basis, the temperature and density dependence of the E_1' annealing can be expected to reflect the variation of O_2 diffusion in the network and consequently yield information on the behavior of the diffusion coefficient.[29,30] Qualitatively one can say that the shift of the annealing curves to higher temperatures as a result of densification (Figs. 3 and 7) indicates a reduction in the diffusion coefficient.

A model specifically applicable to the annealing of defects in a-SiO_2 does not exist at the present time. Various authors[20,27,29,31] have used different models based upon the Waite[30] approach in which randomly distributed interstitial species diffuse to defect sites and anneal them. More sophisticated models using spatially correlated interstitial-defect distributions[32] have also been demonstrated to be applicable.[29,31] To gain some insight into the problem without entering into great depths we use an approximate approach with the Waite model[30] and assume equal densities of defects and interstitial, diffusing species. The diffusion coefficient D can be ascertained from the temperature at which the defect density drops to half its initial value, $C_{E'}^0$,

$$1 = 4\pi r_0 C_{E'}^0 t \left[D + \frac{2r_0\sqrt{D}}{\sqrt{\pi}E} \right] , \tag{3}$$

where r_0 is a capture radius within which distance vacancy-interstital annihilation automatically occurs, t is the anneal time. From the results shown in Fig. 3 for 10-min anneals, and assuming $C_{E'}^0$ has the value $\sim 10^{16}/\mathrm{cm}^3$ in undensified silica and $\sim 10^{18}$ defects/cm^3 in the densified sample, we deduce the activation energy E_A variation:

$$E_A(\text{densified}) - 1.6E_A(\text{undensified}) = 0.28 \text{ eV} ,$$

assuming pre-exponential factors in the diffusion coefficient have not changed. If E_A (undensified) is[25] 1.17 eV, then E_A(densified) is 2.15 eV. Very approximately then, a diffusion-model approach suggests that the activation energy for diffusion of molecular oxygen in the densified samples studied has increased by the order of 1 eV. Note that the possibility of a range of activation energies resulting from the amorphous structure[33] has been neglected and must be included in a proper treatment.

It has been suggested[34,35] that one precursor of the oxygen-vacancy center is the diamagnetic, B_2, center $\equiv \mathrm{Si{=}Si} \equiv$ transforms to the E_1' center by hole trapping:

$$\equiv \mathrm{Si{=}Si} \equiv + e^+ \rightleftarrows \equiv \mathrm{Si}^{+}\mathrm{Si} \equiv \ .$$

To maintain chemical balance, in dry silica, peroxy bridges are proposed[35] to be the partner defects:

$$2(\equiv \mathrm{Si{-}O{-}Si} \equiv) \rightleftarrows \equiv \mathrm{Si{=}Si} \equiv + \equiv \mathrm{Si{-}O{-}O{-}Si} \equiv .$$

Under irradiation the B_2 defects can transform to E_1' defects; however, the present results on unannealed, undensified, and densified dry silica [Figs. 5(d), 5(e), and 5(f)] clearly show that peroxy bridges transforming to peroxy radicals under irradiation do not account for the observed peroxy signals. This may be deduced from comparison of Figs. 5(d) and 5(e), which show that in densified dry silica, irradiation does not produce peroxy signals; annealing after irradiation is necessary [Fig. 5(f)].

The significant increase in E_1' defect creation efficiency in undensified and densified wet silica as compared to dry silica suggests that precursors other than B_2 centers are present. Since it is known[23] that E_1' annealing in wet silica is primarily via diffusion and trapping of H_2O molecules,

$$\equiv \mathrm{Si}^{\cdot} + \mathrm{H_2O} \rightleftarrows \equiv \mathrm{Si{-}OH} + \mathrm{H}^0 \ ,$$

we suggest that the Si—OH bonds formed as growth defects in wet silica act as E_1' precursors. Reduction of Si—OH bonds via the trapping of radiolytic hydrogen and release of H_2O (the reverse of the annealing stage) may be the process of radiation-induced transformation. Furthermore, the apparent absence of peroxy radicals in wet silica (or at least, a very reduced level) may be due to the limited density of O_2 diffusing in wet silica or to the tendency for peroxy linkages to be immediately hydrolized to form OH

bonds to the Si. It remains at first surprising that E_1' defects in both Suprasil I and W1 have essentially the same isochronal anneal curve for the same degree of densification (Fig. 3). We note, however, that in the temperature range 400—500 °C, the diffusion coefficients of O_2 and H_2O in undensified silica are rather similar[25], so that although the annealing species are different, the annealing curves may be not too dissimilar. More-detailed investigation of these points is necessary.

The primary objective of the study undertaken was to try to understand something of the nature of densified silica. It is now clear that a study of the character of the defects reveals little structural information because the spins are highly localized spatially around the defects and consequently insensitive to variations in the environment to first order. Through annealing considerations one can apparently gain some insight into modifications in the network produced by densification. Surprisingly, the ease of creation of both E_1' and NBOH centers in densified silica is dramatically enhanced with respect to the undensified case, even for such densification as small as 3%. We underline the fact that for the γ doses we have used it is unlikely that any degree of defect saturation was attained.[36] The line shapes shown in Fig. 1 and related fit parameters shown in Table II suggest that densification may be accompanied by a degree of local strain. The enhanced radiation sensitivity could then be due to remnant local strain after densification rather than a physical property of the densified state. A picture of densification involving modification of the internal ring structure of the amorphous SiO_2 network and inclusion of local strain then emerges.

ACKNOWLEDGMENTS

The author gratefully acknowledges the help of Professor J. Arndt, who supplied the densified samples, and the Centre d'Etudes Nucleaires de Grenoble, which made available the γ-irradiation facility. Dr. J. Robertson is also gratefully acknowledged for discussions about the problem of defects in amorphous silica.

[1]W. Primak, L. H. Fuchs, and P. Day, Phys. Rev. **92**, 1064 (1953).
[2]W. Primak and R. Kampwirth, J. Appl. Phys. **39**, 5651 (1968), and references therein.
[3]E. P. EerNisse and C. B. Norris, J. Appl. Phys. **45**, 5196 (1974).
[4]R. L. Pfeffer, J. Appl. Phys. **57**, 5176 (1985).
[5]F. J. Feigl, W. B. Fowler, and K. L. Yip, Solid State Commun. **14**, 225 (1974).
[6]W. Primak, Phys. Rev. **110**, 1240 (1958).
[7]K. Vedam, E. D. D. Schmidt, and R. Roy, J. Am. Ceram. Soc. **49**, 531 (1966).
[8]M. Grimsditch, Phys. Rev. Lett. **52**, 2379 (1984).
[9]R. J. Hemley, H. K. Mao, P. M. Bell, and B. O. Mysen, Phys. Rev. Lett. **57**, 747 (1986).
[10]G. E. Walrafen and M. S. Hokmabadi, in *Structure and Bonding in Noncrystalline Solids,* edited by G. E. Walrafen and A. G. Revesz (Plenum, New York, 1986), p. 185.
[11]J. Arndt and D. Stöffler, Phys. Chem. Glasses **10**, 117 (1969).
[12]J. D. Jorgensen, J. Appl. Phys. **49**, 5473 (1978).
[13]R. Couty, Ph. D. thesis, Université Pierre et Marie Curie, 1977 (unpublished).
[14]R. A. B. Devine, I. H. Farnan, R. Dupree, and J-J. Capponi, Phys. Rev. B **35**, 2560 (1987).
[15]F. L. Galeener, Solid State Commun. **44**, 1037 (1982).
[16]J. B. Bates, R. W. Hendricks, and L. B. Shaffer, J. Chem. Phys. **61**, 4163 (1974).
[17]A. G. Revesz and G. V. Gibbs, in *The Physics of MOS Insulators,* edited by G. Lucovsky, F. L. Galeener, and S. T. Pantelides (Pergamon, New York, 1980), p. 92.
[18]F. L. Galeener, R. A. Barrio, E. Martinez, and R. J. Elliott, Phys. Rev. Lett. **53**, 2429 (1984).
[19]R. A. B. Devine, J-J. Capponi, and J. Arndt, Phys. Rev. B **35**, 770 (1987).
[20]A. H. Edwards and W. B. Fowler, Phys. Rev. B **26**, 6649 (1982).
[21]D. L. Griscom, Phys. Rev. B **20**, 1823 (1979); **22**, 4192 (1980).
[22]C. P. Poole, Jr., *Electron Spin Resonance,* 2nd ed. (Wiley, New York, 1983), p. 549.
[23]D. L. Griscom, Nucl. Instrum. Methods B **1**, 481 (1984).
[24]D. L. Griscom, M. Stapelbroek, and E. J. Friebele, J. Chem. Phys. **78**, 1638 (1983).
[25]R. A. B. Devine and C. Fiori, J. Appl. Phys. **58**, 3368 (1985).
[26]D. L. Griscom and E. J. Friebele, Phys. Rev. B **24**, 4896 (1981).
[27]D. L. Griscom, J. Non-Cryst. Solids **68**, 301 (1984).
[28]M. Stapelbroek, D. L. Griscom, E. J. Friebele, and G. H. Sigel, Jr., J. Non-Cryst. Solids **32**, 313 (1979).
[29]R. A. B. Devine, J. Appl. Phys. **56**, 953 (1984).
[30]T. R. Waite, Phys. Rev. **107**, 463 (1957).
[31]R. A. B. Devine, Nucl. Instrum. Methods B **1**, 378 (1984).
[32]H. M. Simpson and S. Sosin, Radiat. Eff. **3**, 1 (1970).
[33]J. F. Shackelford and J. S. Marasyck, J. Non-Cryst. Solids **30**, 127 (1978).
[34]W. B. Fowler, in *Structure and Bonding in Noncrystalline Solids,* edited by G. E. Walrafen and A. G. Revesz (Plenum, New York, 1986), p. 157.
[35]J. Robertson, J. Phys. C **17**, L 221 (1984).
[36]R. A. B. Devine, Appl. Phys. Lett. **43**, 1056 (1983).